Spatial Energy Balancing in Large-scale Wireless Multihop Networks

Seung Jun Baek and Gustavo de Veciana
Department of Electrical and Computer Engineering
The University of Texas at Austin
Austin, TX 78712
Email: {sbaek, gustavo}@ece.utexas.edu

***Abstract*— In this paper we investigate the use of proactive multipath routing to achieve energy efficient operation of ad hoc wireless networks. The focus is on optimizing trade-offs between the energy cost of spreading traffic and the improved spatial balance of energy burdens. We first propose a simple scheme for multipath routing based on node proximity. Then combining stochastic geometric and queuing models we develop a continuum model for such networks, permitting consideration of different types of designs, i.e., with and without energy replenishing and storage capabilities. We propose a parameterized family of energy balancing strategies for grids and approximate the spatial distributions of energy burdens based on their associated second order statistics. Our analysis and simulations show the fundamental importance of the tradeoff explored in this paper, and how its optimization depends on the relative values of the energy reserves/storage, replenishing rates, and network load characteristics. Simulation results show that proactive multipath routing decreases the probability of energy depletion by orders of magnitude versus that of shortest path routing scheme when the initial energy reserve is high.**

I. Introduction

Energy efficient design and operation of ad hoc multi-hop wireless networks is a particularly critical and difficult problem. These problems are heightened in the context of mobile communications systems and/or distributed sensing applications, where energy storage and availability may be quite limited. There are many levels at which one can address this problem. Advances in silicon technology can realize energy savings through power efficient circuitry, e.g., voltage scaling, while specialized architectures can be devised to allow nodes to enter the 'sleep mode'. At the same time power control and optimized MAC protocols can bring substantial energy savings enabling networks with thousands of sensors. Particularly, in large ad hoc wireless networks the data originated from a source might need to be relayed a *long distance* to a destination or sink wireline node. Relaying through many hops causes intermediate nodes to consume substantial amounts of energy and thus make energy efficient routing a particularly critical task.

Consider the network shown in Fig. 1. Two sources $S1, S2$ send to destinations $D1, D2$ on opposite ends of the network respectively. In the network on the left these sessions are supported along shortest hop routes. If one of these sessions were sustained for a long time nodes along the route would eventually see depleted energy reserves, roughly 'dividing' the network into two parts. Subsequently if other nodes need to communicate across this depleted zone they may result in exhaustion of energy along the diagonal, or require selection of routes around this area of the network, which in turn would incur additional energy burdens. This simple example, shows how energy depletion along long routes combined with interactions with future overlapping and/or routing of additional traffic flows might exacerbate the energy problem. A natural solution to this problem is to spread out the energy burden of sustained sessions so as to obtain a more spatially balanced energy burden. Specifically, one may split traffic across two disjoint routes as shown on the right in Fig. 1. Assuming energy consumption is roughly proportional to the load this leads to a more balanced energy burden across sets of intermediate nodes. At the same time this scheme may involve a larger number of nodes, e.g., a route with four versus three hops, and thus an increased overall energy burden.

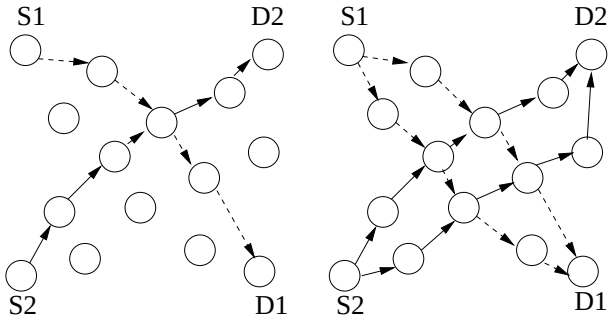

Fig. 1. Comparison of the shortest path routing scheme (on the left) and a typical load-balancing scheme (on the right). The dotted arrows represent flows for $S1 - D1$ and the dashed arrows represent flows for $S2 - D2$, respectively.

In this paper, we consider the system design aspects of such multipath routing strategies associated with a large number of hops – we refer to this as *proactive* balancing of energy burdens over multiple routes. Our primary interest here is not to devise detailed multi-path routing algorithms, but rather to investigate the design and possible improvements afforded by such routing mechanisms. The key intuition is that the more we spread the traffic, the more the energy profile of the network

This work is supported by National Science Foundation under Grant ECS-0225448.

will be balanced. However, a wide spreading will require some packets take long 'detours', which will incur extra energy cost. This tradeoff associated with the degree of spreading is the main topic addressed in this paper.

The paper is organized as follows. In Section II we discuss related work in this area. Section III introduces a concrete multipath routing and balancing strategy, and presents continuum and grid models. In Section IV we characterize spatial energy burdens using a shot-noise process associated with our continuum model. Section V considers a regular grid network, and presents an analysis of a parameterized family of energy balancing strategies. In Sections VI and VII we formulate and investigate the design and optimization of such spreading using second order and asymptotic approximations. Section VIII includes simulation results and a discussion of complex scenarios. Finally Section IX presents our conclusion.

II. Related Work

There has been substantial research on analyzing, designing and implementing energy conserving routing protocols suitable for ad hoc networking applications. Let us highlight a few of these. In [1] a characterization and algorithm determining the most energy efficient route between two nodes is proposed. However, it is not clear whether using such routes extends 'network lifetime,' nor how this would impact network capacity for non-homogenous traffic loads. By contrast, [2] and [3] propose and evaluate routing mechanisms to maximize network lifetime based on nodes' current residual energy reserves. Unfortunately, scalability and the effectiveness of greedy routing to spread energy burdens are a concern. The work of [4] takes yet another tack – they propose packet-level randomized routing in order to proactively balance energy burdens across the network. A unifying principle emerges from this body of work: the tradeoff between minimizing the energy expended to carry an offered load versus the balancing of energy burdens across the network. To the best of our knowledge, the spatial character of this tradeoff has not been studied. The primary contribution of our work is the use of a stochastic geometric framework to analyze, and then work towards realizing this tradeoff in an 'optimal' manner.

III. Spatial Modelling

This section is divided into three parts. We start by stating our model assumptions. Then we introduce a simple multi-path routing scheme based on spatial relationships among nodes. Next, we propose a continuum model where we regard the field of the wireless nodes as the infinitesimal 'medium' that carries fluid, i.e., the traffic flow. This leads to a simple shot-noise process model for the spatial field of energy expenditures which is amenable to analysis.

A. Model assumptions

In this paper we will use a simplified model for energy expenditures associated with data transmissions. Nodes are assumed to share a common transmit power level more than sufficient to guarantee the network is connected. Nodes relay packets towards the destination via *neighboring* nodes in a hop-by-hop manner. We assume that the energy consumption at each node is proportional to the traffic it is carrying, and use the terms 'traffic load' and 'energy burden' interchangeably.

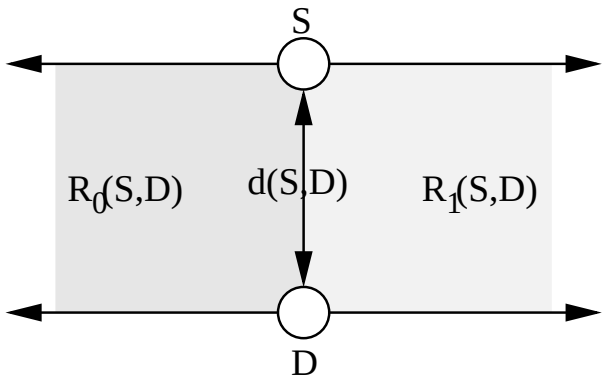

Fig. 2. Illustration of regions $R_0(S,D)$ and $R_1(S,D)$ for the source-destination pair (S,D).

The hop length between every source-destination pair is assumed to be high, i.e., we focus on the spatial energy burden resulting from long routes. In this study we do not explicitly consider energy consumption caused by channel contention. We assume that the network is lightly loaded and transmissions are properly scheduled so that the energy consumption caused by interference and contention is negligible. This simplifies our discussion. The role of the energy burden caused by channel interference and contention is to be included in the future work.

An example which fits our assumptions is an energy-constrained large-scale sensor network with light traffic. Packets generated at a sensor may have to take a large number of hops in order to be delivered to other locations in the network.

Since traffic generated by a node is assumed to be relayed only to its neighbors, the term 'neighbor' needs to be defined precisely. A reasonable choice of neighbors is one based on proximity. We shall model the locations of the nodes as fixed and following a spatial point process in $\mathbb{R}^2$ plane. A natural notion of proximity and neighbor relationship can be introduced via the Voronoi tessellation and Delaunay graphs induced by the locations of the nodes. These are discussed below.

Suppose the locations of the nodes constitute a point process Ψ on the $\mathbb{R}^2$ plane . Each point $x_i \in \Psi$ serves as *seed* for a *cell* $V(x_i)$,

$$V(x_i) = \{y \mid |x_i - y| \leq |x_j - y|, \forall x_j \in \Psi\}$$

in the Voronoi tessellation induced by Ψ. If $V(x_i) \cap V(x_j)$ is not an empty set, we refer to $V(x_i)$ and $V(x_j)$ as *neighboring cells* and we say that x_i and x_j are neighbors.

A *Delaunay graph* is a graph whose vertex set is Ψ and whose edges connect nodes that are neighbors. We denote the Delaunay graph as $G(\Psi, E)$ where E is the set of Delaunay edges. Routes considered in the discussion below will be based on the Delaunay graph and they will be referred to as Delaunay

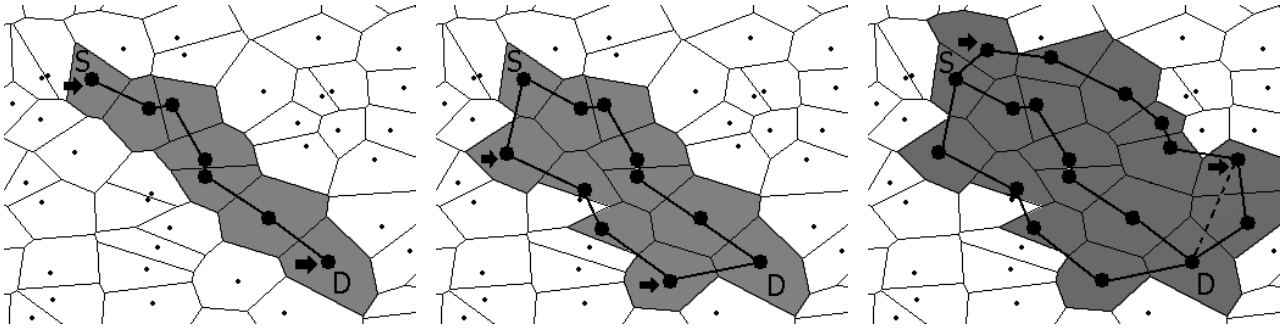

Fig. 3. The figure shows the construction of level 1,2 and 3 routes for nodes S and D, from left to right. The route at each stage is shown with solid lines and the shaded regions are the cells for the nodes in routes. The nodes marked by an arrow are the *connectors* at each route.

routes. We shall assume that the spatial distribution of nodes is fairly uniform and sufficiently dense such that each node can reach its neighbors.

B. A multi-path routing scheme based on the Delaunay graph

Consider a Delaunay route connecting two nodes $x_i, x_j \in \Psi$, and has a minimal length, i.e., sum of the Euclidean length of its edges. This path is referred to as the *Shortest Delaunay Route* (SDR) and its length is a good approximation for the straight line segment that connects x_i and x_j, see e.g., [5], [6]. Note that the SDR is based on the Euclidean norm, thus the SDR may not coincide with the minimum hop route. We will see in the sequel (Section VIII) that this small difference may impact the *distribution* of energy expenditures significantly.

Based on the SDR, we propose the following simple construction to determine a set of additional paths between two nodes, say $S, D \in \Psi$. For purposes of visualizing its spatial characteristics we present a geometric view of this construction :

1) Draw a straight line segment $d(S, D)$ between S and D, and draw two additional lines, through S and D and orthogonal to $d(S, D)$. Let $R_0(S, D)$ and $R_1(S, D)$ denote the open sets above and below the line segment $d(S, D)$, see Fig. 2.
2) We let $N_1(S, D)$ denote the set of nodes included in the SDR from S to D, and refer to this route as the Level 1 route. S and D are referred to as the *Level-1 connectors*.
3) Now find the set of nodes $N_2(S, D)$ which are neighbors of $N_1(S, D)$ and fall in $R_0(S, D)$. Create a route that connects the nodes in $N_2(S, D)$ with Delaunay edges. We refer to the two nodes located at each end of this route as *Level-2 connectors*.
4) Construct a SDR for a Level-2 connector to its closest Level-1 connector and repeat the same for the other connector. if this SDR crosses new nodes, update $N_2(S, D)$ by adding these new nodes in $N_2(S, D)$. Now the nodes in $N_2(S, D)$, S and D can be connected via a Delaunay route which is referred to as *Level-2 route*.
5) Next determine the set of nodes $N_3(S, D)$ which are neighbors of $N_1(S, D)$ but falls in $R_1(S, D)$ this time. Following a similar process as above, find the Level-3 connectors, update $N_3(S, D)$ and construct the Level-3 route.
6) For $w \geq 4$, determine the new set of nodes $N_w(S, D)$ that are neighbors of N_{w-2} and fall in $R_{(w \mod 2)}$. Following the above steps, the Level-w route is recursively constructed.

The basic idea is to recursively construct higher level routes based on nodes which are neighbors of those included in previous levels but alternating between $R_0(S, D)$ and $R_1(S, D)$ in order to balance spreading cost as the levels increase. These routes can be obtained based on a distributed routing scheme since the only information required is the location of neighboring nodes, the source and the destination. We confine relaying nodes to the regions $R_0(S, D)$ and $R_1(S, D)$ so as to prevent routes that extend backward. As will be clear from the construction, the role of connectors is to ensure connectivity via Delaunay routes among S, D and different levels of routes.

An example of our route construction for a source-destination pair (S, D) is illustrated in Fig. 3. At each level, the level connectors are marked with arrows. In the third step, the Level-3 connector and D was not directly reachable via a Delaunay edge (dotted line), thus a SDR between those two nodes is constructed to connect them.

We shall refer to this construction as proximity-based multipath (PBM) routing which gives us a concrete set of paths over which to distribute traffic so as to spread out energy burdens. An approximate model for the multi-path routes by this construction will be considered in Section V.

C. Regular grid and continuum models

As shown in Fig. 3, our multiple routes are spatially clustered. We shall refer to such clusters as the *spatial footprint* of a multipath routing scheme. In order to study the interaction among such footprints given a traffic load, and in particular the spatial energy burdens they induce on the network, we adopt two idealized models.

First, consider a PBM construction in a dense *regular grid network* with each grid dimension is 1×1. The left part of Fig. 4 shows an example of such a construction for several SD pairs. A source transmits a sequence of packets to its destination for some amount of time, and we refer to this process as a *session*. Suppose sessions 'arrive' to and 'depart'

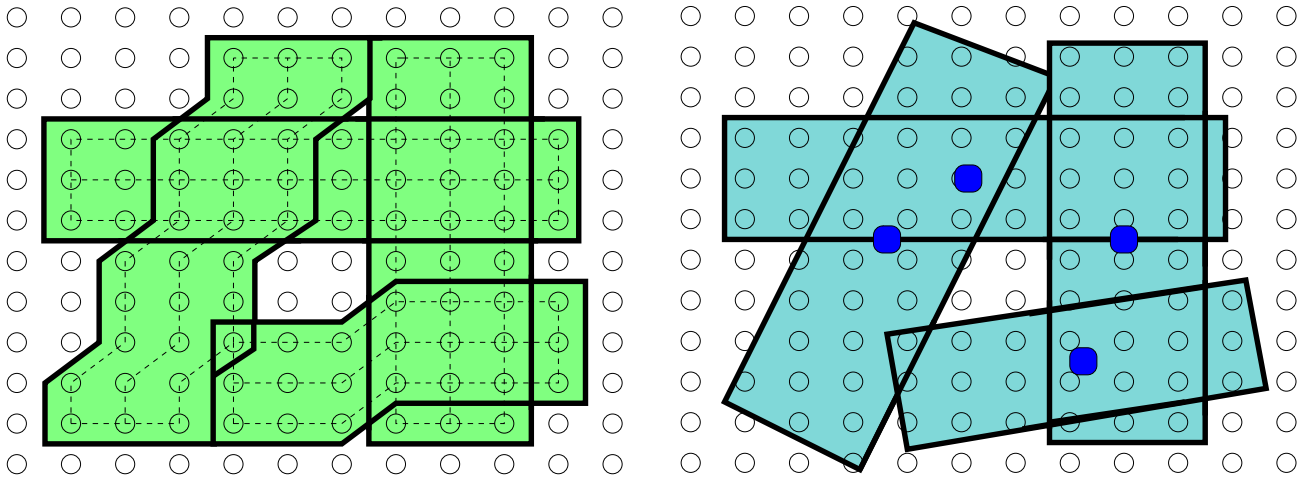

Fig. 4. On the left, the footprints are approximated and adjusted to the grid structure so that the footprints have the regular shape and the topology along the grids. The figure on the right shows the hypothetical square-shaped random sets cast upon the regular grid network.

from the network. Upon departure, each session has depleted, by possibly different amounts, the energy reserves of locations (nodes) traversed by its paths – the session's support set or the *spatial footprint*.

We take a slightly different view of this process. For each node that participates a session, we draw a square or parallelepiped 'cell' of unit area centered at the node depending on the spatial orientation of the session. By merging these cells, we obtain a shaded polygon for each session as on the left of Fig. 4. We assume that the initiation of a session corresponds to the 'arrival' of a polygon into the network and the nodes that fall inside the polygon participate in that session. These nodes comprise the footprint of the session.

Next, we associate each polygon to a random closed set in $\mathbb{R}^2$, e.g., a randomly oriented square as on the right part of Fig. 4. These session arrivals correspond to 'arrivals' of these random sets, e.g., a square on the right of Fig. 4 'generates' a session footprint. Note that the footprint generation process is now reversed, i.e., we assume that there are *a priori* arrivals of random sets in a plane and we 'tailor' each shape to a regular grid structure as an approximation. A possible tailoring of such shape is given by the following procedure.

1) Find the end tip locations of each random square and find the nearest nodes to those points in the grid, mark the nodes as the SD pairs.
2) Draw a regular or parallelepiped square of size 1 around each node such that the node is at the center of each square. Appropriately choose the shape of each square according to the orientation of each footprint: a heuristic example is on the right of Fig. 4.
3) Merge the squares to form footprints around each SD pairs as on the right of Fig. 4.

A careful comparison of the examples in Fig. 4 should give the idea.

For purposes of modelling the dynamic spatial behaviors of these random sets, we assume that the *geometric center of mass* of each random set 'falls' into a $\mathbb{R}^2$ plane whose

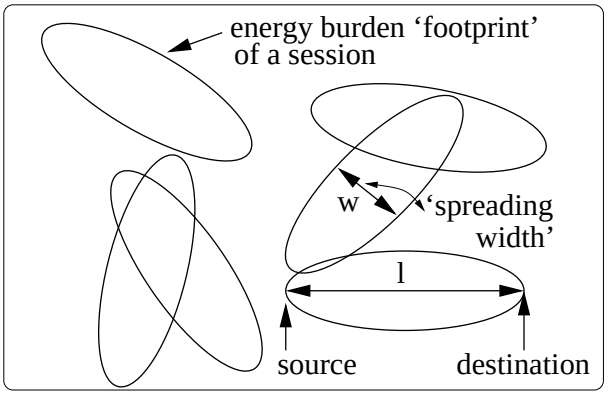

Fig. 5. A realization of the energy footprints for sessions in ad hoc network. A footprint is assumed to have elliptical shape for the purpose of illustration.

collection constitutes a spatial-temporal point process. As an example, see the right of Fig. 4 where the black dots represent the center of masses for various footprints.

Next we introduce a continuum model. Consider the limiting process of the above construction such that the density of the nodes becomes very large. We can think of an infinitesimal area in space as corresponding to a node with some initial energy reserves. Fig. 5 exhibits a realization of the process capturing the energy burdens incurred over a period of time – only sessions' footprints are shown. As shown in Fig. 5, every footprint is assumed to have some well-defined, possibly random, *continuum* shape. Here the footprint itself plays the same role as the random sets in the previous grid model. The source and destination nodes are located at each end of the footprints. Here we denote the 'length' of a footprint which corresponds to the distance between a SD pair as l, and the maximum 'width' of a footprint which is related to the *spreading factor* as w.

Each location within a footprint corresponds to a infinitesimal node which may experience different amount of

load/energy burden. Since the footprint is a random closed set in $\mathbb{R}^2$, we shall define a *load distribution* function that maps a point in the footprint to the relative load intensity it sees. Essentially such load distribution function depends on (1) a particular strategy of 'spreading' traffic within a footprint, (2) the degree of spreading, w and (3) the connection length l. We will characterize the relevance of these parameters to the energy burden profile in a network in the rest of this paper. Let us assume that every SD pair carry the same amount of traffic. Intuitively, the footprints associated with a larger w and the same l occupy more area, but the energy load per unit area would be lessened – this will be further quantified in the following sections.

As this model suggests, it is natural to introduce a *shot-noise process* in $\mathbb{R}^2$. Footprints are associated with a point process corresponding to the collection of centers of masses, and each footprint contributes to energy burden at certain location depending on its shape and load distribution function. Furthermore, if multiple footprints overlap at a location, the burden at that location is an *additive* one contributed by the overlapping footprints. We will use the shot-noise model to capture spatial characteristics of the energy burden, and later, a regular grid model to parameterize such characteristics for system design purposes.

IV. Characterization by Continuum Model

A. Shot-noise formulation

The continuum model proposed in the previous section can be mathematically formalized as a shot-noise process. Let Φ_0 denotes a random closed subset of $\mathbb{R}^2$ corresponding to taking a fixed shape (footprint) with center of mass at the origin and a random rotation in $[0, 2\pi)$. We will refer to Φ_0 as the distribution of a typical footprint. The energy burden for an infinitesimal region (node) falling within the footprint is modelled as follows. We define the *load distribution* function $h(\cdot, \Phi_0) : \mathbb{R}^2 \to \mathbb{R}_+$ as giving the energy burden, such that, for $y \in \mathbb{R}^2$, if $y \notin \Phi_0$ then $h(y, \Phi_0) = 0$ and otherwise $h(y, \Phi_0)$ assumes some nonnegative value corresponding to the energy burden in an infinitesimal spatial area located at y for a footprint Φ_0 *centered at the origin*.

We assume that the centers of mass of sessions constitute a spatio-temporal Poisson point process Π with intensity $\lambda(x, t)$ at location x and at time t. Let us denote by Π_t a *spatial* point process in $\mathbb{R}^2$ for the centers of the sessions/footprints that have been been offered to the network prior to time t. Thus Π_t has the spatial intensity of $\int_0^t \lambda(x, u)du$ at location x. Each point $x_i \in \Pi_t$ has an associated footprint denoted by Φ_i. We assume $\{\Phi_i\}$ are i.i.d. copies of Φ_0 and are invariant to shifts in $\mathbb{R}^2$ for all x_i. Thus the contribution of the energy burden on location x from the session at x_i with Φ_i, will be $h(x - x_i, \Phi_i)$. Note since we equivocate load and energy burden, $h(\cdot, \Phi_i)$ depends on how a routing mechanism chooses to spread flow of session i within its footprint Φ_i.

Suppose that all the nodes initially have identical energy reserves at time 0. Then the total energy burden accumulated at location $x \in \mathbb{R}^2$ has a shot-noise representation given by

$$G(x, t) = \sum_{x_i \in \Pi_t} h\left(x - x_i, \Phi_i\right). \tag{1}$$

For simplicity, we assume that Π is a Poisson process, homogeneous in time and space with the constant intensity λ per unit time per unit area. Then Π_t is a homogeneous Poisson point process with intensity λt. Next we state several known results from the shot-noise theory. Since Π_t is stationary, we can consider a typical node as being at the origin to obtain the following result.

Lemma 1: (See [7].) Let us define $G_0(t) := G(O, t)$, the energy burden at the origin. Also let $\chi^{(n)}(t)$ be the nth order cumulant of $G_0(t)$. By the homogeneous Poisson property of Π_t, we have that

$$\chi^{(n)}(t) = \lambda t \; E\left[\int_{\Phi_0} h(x, \Phi_0)^n dx\right].$$

Define the normalized mean μ and variance σ^2 as:

$$\mu := \; E\left[\int_{\Phi_0} h(x, \Phi_0) dx\right], \tag{2}$$

$$\sigma^2 := \; E\left[\int_{\Phi_0} h(x, \Phi_0)^2 dx\right]. \tag{3}$$

Then we have that

$$E[G_0(t)] = \lambda t \mu,$$
$$\mathrm{Var}[G_0(t)] = \lambda t \sigma^2.$$

As mentioned earlier, the function $h(\cdot, \Phi_0)$ captures both the 'shape' and how the flow is spread within a typical footprint. Thus it is one of the design choices one can make to control the mean and variance of the energy burdens. Although using only these two moments to describe the statistical properties of $G_0(t)$ may not be sufficient, the following theorem shows that it can be a good approximation (see [7]).

Theorem 1: (Asymptotic normality of shot-noise process) *Consider $G_0(t)$ defined in Lemma 1. We have that*

$$\frac{G_0(t) - \lambda t \mu}{\sqrt{\lambda t} \sigma} \xrightarrow{d} N(0, 1) \;\; \textit{as} \;\; t \to \infty$$

where $N(0, 1)$ is the standard normal distribution.

From this theorem, we have that, for large t, the probability of energy burden exceeds a prescribed level b is given by

$$P(G_0(t) > b) \quad \simeq \quad \phi\left(\frac{b - \lambda t \mu}{\sqrt{\lambda t} \sigma}\right), \tag{4}$$

$$\phi(u) \quad := \quad \frac{1}{\sqrt{2\pi}} \int_u^\infty e^{-v^2/2} dv. \tag{5}$$

Without loss of generality, let us assume $\lambda = 1$ throughout the rest of the paper. In order for t to be effectively large, we need a typical node in the network to see a large number of footprints that overlap on average. For example, if the typical footprint has fixed, rectangular shape with its length $l = 20$ and spreading factor $w = 5$, then a typical point in the field

experiences the overlapping of 100 footprints on average when $t = 1$. Thus the distribution of energy burden may be safely assumed to be roughly normal even for moderate values of t.

B. Depletion probability, network lifetime and variance-optimal schemes

A common criterion for energy performance of a network is lifetime, e.g., the time before some fraction of nodes will be below a certain battery level. Our objective lies in the complementary question: given a *desired network operation time*, how can we minimize the fraction of the depleted nodes? For example, if one wishes to operate a sensor network for a week, what fraction of nodes are expected to survive during a week and what is a proper multi-path routing strategy to achieve this? We believe this problem is of more practical interest in engineering such networks. To address the above question, we shall use the normal approximation in Theorem 1.

Let τ be the desired time for network operation. Then the fraction of nodes that have not exceeded the critical level b during τ is given by

$$\phi\left(\frac{b-\tau\mu}{\sqrt{\tau}\sigma}\right). \tag{6}$$

Suppose the critical reserve level b is specified as a multiple k of $\tau\underline{\mu}$ which is defined as the mean energy consumption of the *baseline* scheme, i.e., a scheme without multi-path routing. Thus the critical level b is specified in terms of a factor k times the mean energy consumption of baseline scheme during τ. Thus $b = k\tau\underline{\mu}$ and let us define $z_k(\tau)$ as follows.

$$z_k(\tau) := \sqrt{\tau}\,\frac{k\underline{\mu}-\mu}{\sigma}. \tag{7}$$

Thus to reduce depletion we wish to maximize $z_k(\tau)$ for a given τ, i.e., minimize the probability of depletion $\phi(z_k(\tau))$ by changing μ and σ.

Eq. (7) provides us with crucial insights. Certainly we would like to minimize both μ and σ, however as we will see later that there is a *tradeoff* between these parameters, i.e., we can decrease μ at the cost of increasing σ, and vice versa. The optimal tradeoff will depend on k. If $k\underline{\mu}$ is small, one might try to decrease μ. Conversely, if k is relatively large, one might prefer strategies that give smaller σ.

In our study we focus on schemes that minimize σ^2, i.e., *variance-optimal strategies*. Thus we assume k is moderately large, i.e., all the nodes have sufficient energy reserves in the beginning so that they do not suffer from depletion when only a few sessions overlap a given location. However, the significance of such variance optimal strategies does not come only from such assumption. From (7), we see that σ has *multiplicative* factor on $z_k(\tau)$ and in [8] we show that variance optimal schemes yield values that are very close to the optimal $z_k(\tau)$ even for no large values of k.

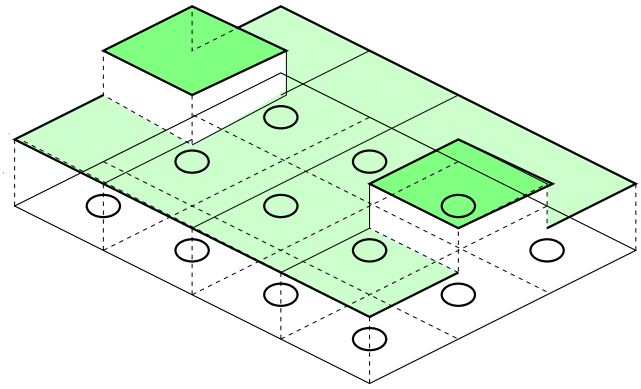

Fig. 6. The function $h(\cdot,\Phi)$ where Φ is the whole square area that contains the nodes represented by circles and $h(\cdot,\Phi)$ takes the continuous values represented by the heights of the shaded region.

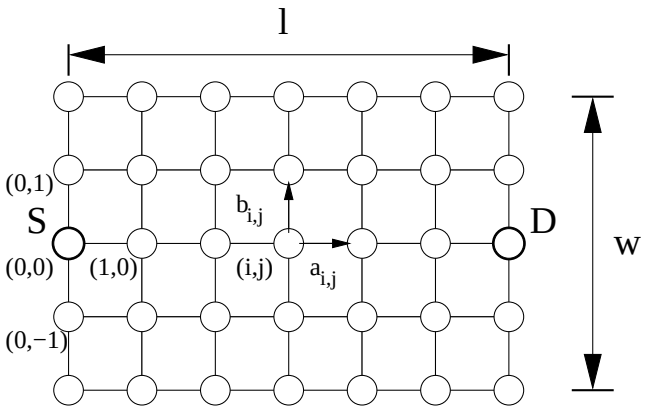

Fig. 7. Topology of the regular grid footprint. The coordinates of locations are shown for some nodes in their lower left corners. The source and the destination is marked by S and D respectively and the dimensions, l and w, of the grid are shown.

V. Parametrization by Grid Model

In this section we revisit the regular grid model proposed in Section III to study flow distribution that minimize σ^2. Nodes are assumed to be tiled to form a regular grid where the spacing among the nodes is 1. To be consistent with our continuum model, Φ_0 represents the typical random set inducing a footprint, e.g., a square on the right of Fig. 4. The load distribution $h(\cdot,\Phi_0)$ is now given as a continuous function taking values of the allocated rate at each node and assuming the form of step functions as shown in Fig. 6. In the figure, the heights represent the values of such rates and $h(\cdot,\Phi_0)$ is constant within a grid square where the random set Φ_0 is the whole square area containing the nodes. The integrations in (2) and (3) can be approximated as *summations* of traffic load at each node. Thus the problem reduces to a flow distribution on a grid. With these assumptions on $h(\cdot,\Phi_0)$, we derive the expressions of (2) and (3) suited for the grid model.

Assume that Φ_0 is a rectangle of dimension $l \times w$ where l and w are assumed to be fixed for the present, and has random rotation uniformly distributed in $[0, 2\pi)$. In spite of its random rotation, we assume Φ_0 approximately covers a footprint of

length l grid steps and the maximum width of w grid steps by the argument of 'tailoring' random sets to grid structure in Section III.

A footprint is defined as the set of nodes in the grid that carry nonzero flow, and its shape is shown in Fig. 7. We assume w is an odd integer to maintain the symmetry, and that it does not exceed l, which is reasonable since spreading beyond l is not likely to be useful, which will be shown later.

We introduce some notation. We label each node with an integer coordinate (i, j) placing the source node at the origin as shown in Fig. 7. The horizontal flow rate from node (i, j) to $(i+1, j)$ is denoted by $a_{i,j}$ and the vertical flow rate from node (i, j) to $(i, j+1)$ is denoted by $b_{i,j}$. We denote the flow or the energy consumed at node (i, j) by $e_{i,j}$, i.e., $e_{i,j} := a_{i,j} + b_{i,j}$.

Define the set $H := \{(i, j) \mid 0 \le i \le l,\ |j| \le (w-1)/2\}$. Under the above construction, we have that

$$\mu = E[\int_{\Phi_0} h(x, \Phi_0)dx] \approx \sum_{(i,j)\in H} e_{i,j}, \tag{8}$$

$$\sigma^2 = E[\int_{\Phi_0} h(x, \Phi_0)^2 dx] \approx \sum_{(i,j)\in H} e_{i,j}^2, \tag{9}$$

We wish to minimize (9) by properly setting $a_{i,j}$ and $b_{i,j}$ for given w and l.

Suppose that the flows are symmetric with respect to $i = \frac{l}{2}$ axis and $j = 0$ axis where l is assumed to be an even integer for simplicity. Especially we refer to the axis $i = \frac{l}{2}$ as the middle abscissa, abbreviated as MA.

We formally define the variance optimal flow distribution problem as:

Problem 1:

$$\textit{Minimize: } \sum_{i,j\in H} e_{i,j}^2 = \sum_{i,j\in H} (a_{i,j} + b_{i,j})^2. \tag{10}$$

Constraints:

$$a_{i,j} + b_{i,j} = a_{i-1,j} + b_{i,j-1}, \tag{11}$$

$$a_{0,0} + b_{0,0} = 1, \tag{12}$$

$$a_{i,j},\ b_{i,j} \ge 0,$$

$$a_{l/2,j} > 0,\ \textit{for } j = \pm(w-1)/2, \tag{13}$$

Variables: $a_{i,j},\ b_{i,j}$.

where (11) corresponds to the flow conservation at each node, (12) the source emitting 1 unit of flow, and (13) the definition of a footprint.

In addition to flow conservation, note the (11) also assumes that the flow routed for the nodes to the left of MA moves away from the source, and at the nodes to the right of MA towards the destination. This ensures that traffic does not flow in an inefficient manner where energy is wasted without reducing variance. Constraint (13) comes from the specification of the width w of the footprint, i.e., the maximum width that the nonzero amount of flow can be spread over.

Standard optimization techniques such as the projected gradient method [9] can be applied to solve Problem 1. However

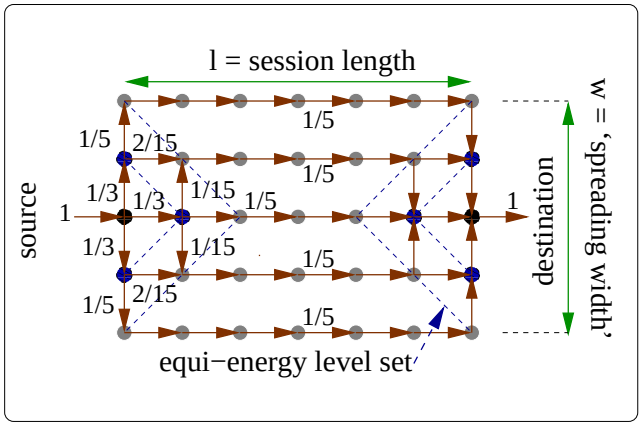

Fig. 8. The optimal flow allocation when $w = 5$ and $l = 7$.

we will simplify the problem by adding an extra constraint of

$$a_{l/2,k} = \frac{1}{w},\ (|k| \le (w-1)/2), \tag{14}$$

i.e., the flow rates are equal along the MA. Our rationale is that, first, this yields a closed-form, simple and intuitive solution. Second, it gives a good approximation especially for large values of l. In [8], we show that the solution obtained for the suboptimal scheme converges to the optimal solution when l is large.

For the modified problem, the solution can be obtained by exploiting the convex characteristic of the objective. Also note that it suffices to specify $e_{i,j}$ as the solution, since it can be shown that by solving $e_{i,j}$ and the constraints, we can obtain $a_{i,j}$ and $b_{i,j}$ for all (i, j).

Lemma 2: The solution to Problem 1 with the additional constraint (14) is, for all $(i, j) \in H$,

$$e_{i,j} = \begin{cases} \{2(|i| + |j|) + 1\}^{-1}, & |i| + |j| \le \frac{w-1}{2}, \\ \{2(|l-i| + |j|) + 1\}^{-1}, & |l-i| + |j| \le \frac{w-1}{2}, \\ w^{-1}, & \text{otherwise.} \end{cases}$$

Proof: See appendix. ■

An example of such a flow assignment is illustrated in Fig. 8. The dotted lines are contours that represent level sets of nodes which have the same total flow. The value of the levels decreases harmonically, i.e., $(1, \frac{1}{3}, \frac{1}{5}, \ldots)$ as the contour expands outward from the source. All $a_{i,j}$ and $b_{i,j}$ are specified in the figure.

For this flow assignment, we have that

$$\mu \approx \sum_{(i,j)\in H} e_{i,j} = l + \frac{w}{2} - \frac{1}{2w}, \tag{15}$$

$$\sigma^2 \approx \sum_{(i,j)\in H} e_{i,j}^2 = \frac{l}{w} - \frac{1}{2}\left(1 + \frac{1}{w^2}\right) + \sum_{k=1}^{\lfloor \frac{w+1}{2} \rfloor} \frac{2}{2k-1}. \tag{16}$$

The following observations are in order. For $1 \le w \le l$, we see that μ increases with w, i.e., the mean energy increases with the spreading width, since the flow travels longer distances. However, σ decreases with w, i.e., the variance

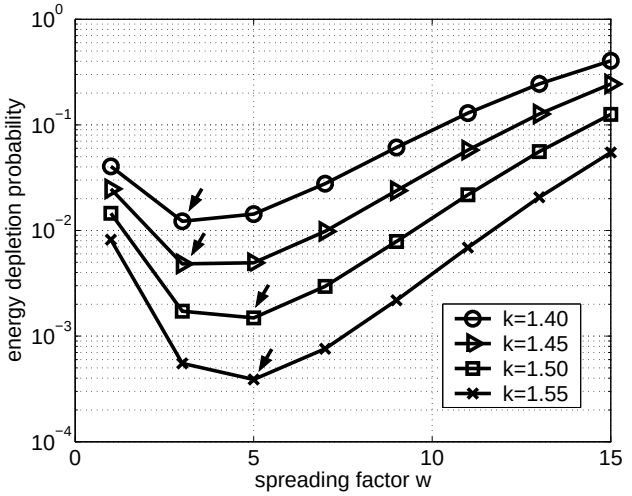

Fig. 9. A numerical evaluation of optimal design of spreading parameter by the regular grid spreading strategy discussed in Section V. The hop length l is fixed to 20 and the initial energy reserve parameter k is varied. Note the change in the tradeoff points marked by arrows, i.e, the optimal w moves from 3 to 5 with increasing k.

decreases with the degree of spreading. Thus one cannot minimize the mean and the variance simultaneously. Also if w is large such that it is comparable to l, the cost of spreading will reduce the benefits of spreading.

The interesting case is where l is much larger than w. Clearly, the mean energy is roughly invariant for small changes in w, but the variance is sensitive to w – the dominant term $\frac{l}{w}$. Thus for a load that traverses a long route, the benefit from spreading is large. For detailed discussion, we refer the readers to [8].

VI. Design Tradeoffs: Networks without Energy Replenishing Capability

A. Depletion probability of the typical node

In this section we numerically evaluate the depletion probability of the typical node, combining the estimates (15) and (16) with $z_k(\tau)$. Here τ is assumed to be 1 and l is set to 20. Fig. 9 exhibits a plot of $\phi(z_k(\tau))$ for varying k, i.e., varying the initial energy reserve of the network versus the spreading factor w. Clearly, there exists w that minimizes the depletion probability for each k: see the points marked by arrows. As expected, for the case where nodes have more initial energy reserves, we should use a larger w. The intuition is that, whenever the nodes in the network have large residual reserves, they should cooperate to balance load on the network, i.e., increase the nodes participating in carrying a flow, but up to certain degree the load balancing itself does not overload the network.

B. Depletion probability of the maximum burden node

As a consequence of the previous normality result, we can also approximate the spatial energy burden pattern as a stationary, isotropic Gaussian random field in $\mathbb{R}^2$. Consider $G(x,t)$ in (1) for $x \in \mathbb{R}^2$. We assume the whole network occupies a region $A \subset \mathbb{R}^2$. Consider the probability that the node with the highest energy burden exceeds the prescribed level b, i.e.,

$$P(\sup_{x\in A} G(x,t) > b). \tag{17}$$

We can estimate the asymptotic value of this probability as $b \to \infty$ via extreme value theory for homogeneous Gaussian fields, e.g., [10], [11]. Denote the desired network operation time by τ as before, and consider the normalized energy burden $Z(x,t) := (G(x,t) - t\mu)/\sqrt{t\sigma}$ where $\lambda = 1$. Let us assume that at τ, we have a spatial covariance function $r_\tau(y)$, i.e., $r_\tau(y) = E[Z(x+y,\tau)Z(x,\tau)]$ for some y. Since the field is isotropic, this function depends only on the norm of y, denoted by $|y|$. Suppose that the following holds for some positive constant a, and for y with very small $|y|$.

$$r_\tau(y) \approx 1 - a|y|^\alpha \text{ , as } |y| \to 0.$$

Here α denotes the infinitesimal order of decay of the covariance with the distance $|y|$. Again assume that b is given by $k\mu\tau$ where k is large, then based on the Poisson clumping heuristic [11], we can rewrite and approximate (17) as follows.

$$P(\sup_{x\in A} Z(x,\tau) > z_k(\tau)) \approx H_\alpha |A| a^{2/\alpha} \{z_k(\tau)\}^{4/\alpha} \phi(z_k(\tau)) \tag{18}$$

where $|A|$ is the area of the region A and $H_\alpha > 0$ is the 2-dimensional Pickand's constant which depends only on α. We see that the depletion probability is proportional to the physical area of the network, and is related to the covariance structure of the footprints. Comparing with the analysis for typical node case, we have the common term $\phi(z_k(\tau))$, but there is the extra term $\{z_k(\tau)\}^{4/\alpha}$ which gives an additional penalty when $z_k(\tau)$ is large.

Thus we expect that, by increasing w, the overall rate of decay in covariance will decrease and one will observe a similar tradeoff as seen earlier in Fig. 9, but the curve will be *flatter* due to the penalty term. This has been verified by using numerical evaluation along with estimation of a, α and $z_k(\tau)$. For details we refer the reader to [8].

VII. Design Tradeoffs: Networks with Energy Replenishing Capability

Next we consider the case where nodes have capability of replenishing their energy at constant rate of c units per unit time. The energy storage capacity of each node is b. We model the energy level of a node by a queue where arrivals correspond to energy burdens which are served, i.e., replenished at rate c. Note that the dynamics of the queue and their physical interpretations are reversed: 'filling' the queue with energy burden corresponds to 'consuming' its energy reserves. Thus, we are interested in the likelihood that the queue length exceeds the level b. We consider two regimes as follows.

A. Nodes with small initial energy reserves

Suppose first the initial energy reserve is small relative to the typical energy expenditure of a node. Thus we might conservatively study the case where the reserve at any point in time is virtually zero. Consequently, it is necessary that the instantaneous cumulative energy burden on a typical node does not exceed the *rate of replenishing*. Thus we estimate the probability that an excessive instantaneous energy burden is seen at a typical node. The spatial energy burden per unit time is simply a shot noise process with the spatial density of λ. Thus a design goal would be, for given threshold probability δ and at typical location x, that

$$P(\sum_{x_i \in \Pi_1} h(x - x_i, \Phi_i) > c) < \delta \tag{19}$$

which can be estimated by using Chernoff bound combined with (15) and (16). We leave this to consider the more interesting case where nodes can store and replenish their energy reserves.

B. Nodes with large initial energy reserve and small replenishing rate

In this regime the energy replenishing rate of a node is much smaller than the rate of consumption, but nodes have large energy storages. Consider a typical node covered by multiple session footprints. The energy load requests for each footprint is buffered into the node's energy queue which is replenished at rate c. An energy request fills the queue, i.e., consumes energy at a constant rate. This can be modelled by using a continuous load model such as fluid queues, e.g., see [12]. However, since the energy consuming rate is assumed to be much greater than the replenishing rate, we can assume that energy burdens are offered *instantaneously* to nodes. Also the offered load at the typical node depends only on its location within the footprints that 'hit' the location. Furthermore, footprint arrival process is assumed to be a homogeneous Poisson process in time and space. Thus an $M/GI/1$ queue can be used as an approximate model.

In this regime, we intend to find the *asymptotic decay rate* of the queue content which is an indicator of the probability that the energy burdens exceed a large initial energy reserve of b. For a stable, single-server queue, we denote the steady-state workload by W. If the following condition is satisfied for some $\theta^* > 0$:

$$b^{-1}\log\{P(W > b)\} \overset{b\to\infty}{\to} -\theta^*,$$

then we refer to θ^* as the asymptotic decay rate [13]. We use the results in [13] to describe the behavior of the tail probabilities.

Let us define the problem. The amount of energy requests are assumed to be i.i.d. but its distribution is not heavy-tailed since every footprint is assumed to occupy a finite area. We denote the virtual workload for the energy queue at time slot $(i, i+1]$ for $i \in \mathbb{Z}$ as W_i . Then we have that

$$W_{i+1} = \max[W_i + X_{i+1}, 0] = \sup[W_i + X_{i+1}]^+,$$

where $X_i = S_i - c$ and S_i is the total energy burden per unit time slot, and c is the replenished energy per time slot. These dynamics correspond to a Lindley process, and since X_i are i.i.d., we can readily apply the following results on the decay rate function.

Theorem 2: [13] *Let us assume $\{W_i\}$ is stationary and thus stable under condition $E[X_i] < 0$, i.e., $E[S_i] - c < 0$. If $\{X_i\}$ are i.i.d., then θ^* satisfies*

$$\rho(\theta^*) = 0, \ \frac{d}{d\theta}\rho(\theta^*) > 0$$

where $\rho(\theta) = \log E[e^{\theta X_i}]$.

We can readily obtain the required cumulant generating function as follows.

Theorem 3: The cumulant generating function $C(\theta)$ of S_i is given by

$$C(\theta) = \log E[e^{\theta S_i}] = \lambda E[\int_{\Phi_0} \{e^{\theta h(x,\Phi_0)} - 1\} dx].$$

Hence we have the rate decay function $\rho(\theta)$ is given by

$$\rho(\theta) = \lambda E[\int_{\Phi_0} \{e^{\theta h(x,\Phi_0)} - 1\} dx] - c\theta$$

under the stability condition

$$\lambda E[\int_{\Phi_0} h(x, \Phi_0) dx] < c. \tag{20}$$

Proof: See appendix. ■

The stability condition relates the replenishing rate c, and the rate of new requests per unit area, λ, times the average total energy request within a footprint. The root θ^* of $\rho(\theta) = 0$ may be found numerically. Using expressions (15) and (16) and the regular grid approximation, some decay rates with varying spreading factors are given in Table I. Here $l = 8$ and $\lambda = 1$, and let us denote the critical replenishing rate to satisfy the stability condition when $w = 7$ as c^*. The replenishing rate c is set to βc^* where $\beta = 1.2$ and 2.0.

Again we observe the tradeoffs associated with different rates of replenishing. When $\beta = 1.2$, the optimal spreading factor is 3. Meanwhile, with a higher replenishing rate of $\beta = 2.0$, the optimal w is increased to 5. The intuition here is that, with higher replenishing rates, one can spread traffic further to enjoy the spatial balancing effect. However, if the replenishing rate decreases close to the critical value, the mean energy cost to spread is no longer negligible so that smaller spreading factor is preferred.

TABLE I
DECAY RATES WITH VARYING SPREADING FACTORS

Spreading factor	Decay rate θ^*	
w	$\beta = 1.2$	$\beta = 2.0$
1	0.8673	1.7125
3	**1.2506**	2.7080
5	1.0965	**2.7593**
7	0.7965	2.6831

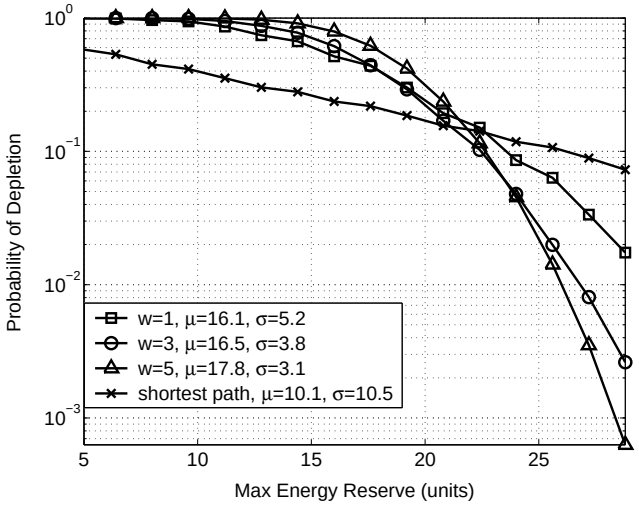

Fig. 10. Energy depletion probability for nodes without energy replenishing capability. μ and σ represents the mean and the standard variation of energy expenditure of each scheme.

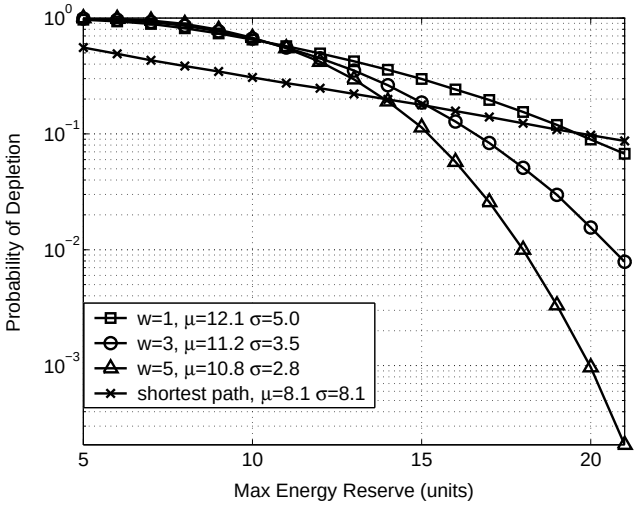

Fig. 11. Energy depletion probability for nodes with energy replenishing capability.

VIII. Simulations

A. Basic setup

In this section we simulate several scenarios to further explore the benefits of proactive spreading. We will deal with stateless routing schemes, however we extend the idea of proactive spreading to routing schemes with states, e.g., a routing depending on nodes' residual energy reserves. The performance metric is evaluated given a maximum energy reserve (MER), what would be the probability that a randomly selected node is depleted of its energy reserve. This metric is of fundamental importance in an engineering perspective, since for a given network operation time and a MER, we may wish to find out the probability of a typical node having depleted of its reserves, or equivalently, the fraction of depleted nodes in the network.

An average of 400 node locations are generated on a 20×20 unit square according to a homogeneous Poisson point process with intensity 1. Session arrivals are homogeneous in space, and a total of 200 sessions are offered at each simulation. Each session offers 1 unit of load per unit time with a (random) holding time of 1 unit time (on average). We simulate session arrivals by picking two nodes at random, which are given by source-destination pair and then setting up a unidirectional flow. We have used PBM route construction introduced in Section III, and the flow is equally divided to each path in order to approximate the scheme in Section V. Note that in our simulation, the 'shortest path routing' (SPR) is a routing that takes the minimum number of hops on the Delaunay graph of nodes. This must be distinguished from the shortest Delaunay routing (SDR) which is a PBM routing without spreading, or equivalently, with the spreading factor w of 1.

B. Scenarios

1) Nodes without replenishing capability: Fig. 10 shows the average energy depletion probability for several values of the spreading factor w along with the shortest routing scheme. A point (x, y) in this plot is interpreted as follows: 'the probability that the energy expenditure of a typical node *will exceed* x is y'. If x is the MER, y is the probability that a typical node is depleted.

Let us consider only proactive routing first. When the MER is less than roughly 20 units, routing with a minimal spreading factor $(w = 1)$ performs best. However, as the MER increases to more than 25 units, proactive multipath routing with the largest spreading factor $(w = 5)$ outperforms the others. These results are consistent with previous discussions, since if we have the high MER we prefer a scheme with a lower variance in the energy expenditure $(w = 5)$ at the cost of higher mean energy expenditure, and vice versa. These tradeoffs occur when the maximum reserve is between 20 and 25 units in our simulation. The SPR has a lowest mean energy expenditure but with the highest variance, and suffers from the worst performance in 'tail behavior', i.e., the lowest slope in the decay for the probability of depletion with the MER. Also note that it has different performance as compared to the SDR $(w = 1)$ case: the SDR performs better due to its steeper slope in the tail probability. We verified that, for SDR, the shape of the empirical histogram of energy burden indeed resembles the Gaussian p.d.f., meanwhile for the SPR we see a monotonically decreasing shape with a heavy tail [8].

2) Nodes with replenishing capability: Fig. 11 shows the energy depletion probabilities when the nodes have the capability of replenishing their energy reserves. Here each connection arrives to the network with interarrival time is randomly distributed in $[0, 1]$ time unit and has replenishing rate of 0.125 energy units per unit time. The benefit from the proactive spreading is greater than that seen for the non-replenishing case. The intuition here is that, for larger w, the average number of nodes that participate in a session is greater than that of a scheme with less w. Thus more nodes have a chance to replenish their energy reserves, which results in a reduced

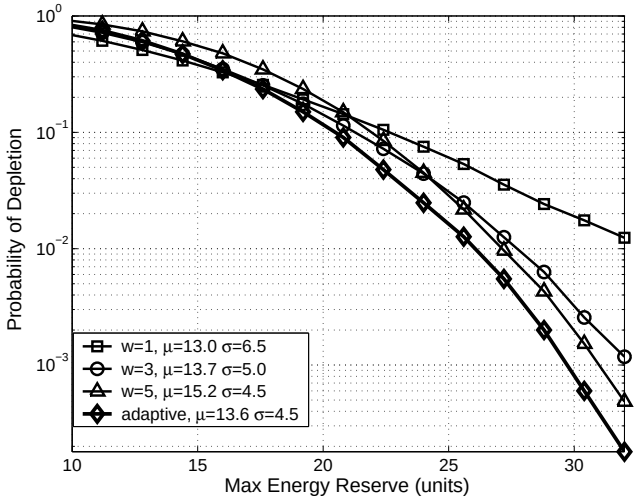

Fig. 12. Energy depletion probability for the dynamic spreading scheme adjusted to session load and hop length.

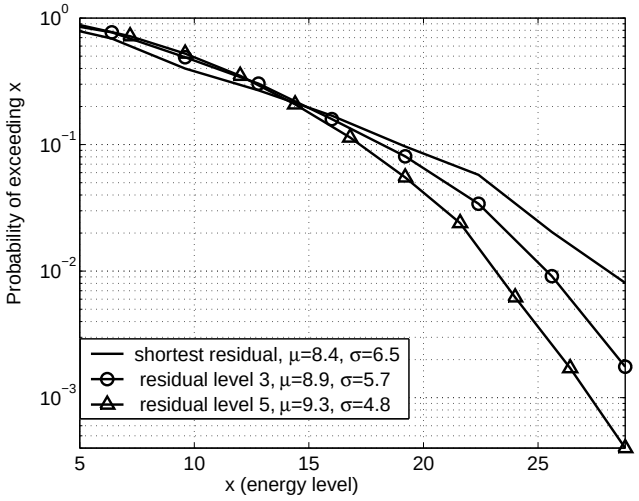

Fig. 13. Comparison of the shortest residual routing, the level-3 and the level-5 residual routing.

mean *and* less variance in the energy expenditure (see μ and σ in the legends) with the largest spreading factor, $w = 5$.

3) Adaptive spreading: Can we dynamically assign 'proper' spreading factor for sessions with different ranges (distance between source and destination) and loads? Intuitively, for a session with longer range and larger load, one should spread more. Let us denote the range and load of a session, possibly random, as L and D. In fact, we find that the optimally assigned spreading factor is approximately proportional to $\sqrt{LD}$ *irrespective of the distributions of* L *and* D. (see [8]). Fig. 12 shows the simulation results of such an adaptive spreading scheme. Here each session carries i.i.d. exponentially distributed load of mean 1. As shown in the figure, the adaptive scheme provides the superior performance over the schemes with the fixed spreading factors.

4) Routing based on residual energy reserves: Here we consider a different class of routing schemes and study how it benefits from proactive load balancing. Specifically we consider the routing scheme based exploiting knowledge of the residual energy reserve at each node, i.e., routing with state information. We use Bellman-Ford algorithm for the minimum cost routing, where the cost is a decreasing function of the fraction of the residual energy to its full capacity. In this way, a route with relaying nodes having relatively high energy reserves will be preferred even if that route involves a higher number of hops. Specifically, if the residual energy of ith node is $b_i(t)$ at time t, the cost of routing traffic to that node is $(b_i(t)/b_{max})^{-\gamma}$ where γ is some positive constant and b_{max} is the maximum energy reserve at a node. As for the choice of γ, a related study [14] shows that a value within the range of $0.5 \sim 2.5$ is preferable. We have chosen $\gamma = 1$. Also, we have assumed that the routes do not change once created. Of course, one can think of a scenario where the routes are updated, adapting to changes in energy reserves of the neighboring nodes. We exclude such functionality, since the scheme can suffer from a severe scalability problem due to the large number of the nodes.

In our simulations, we define a level-w residual routing to be such that, the w best disjoint routes are chosen and flow is spread as done earlier. Fig. 13 shows one of such comparison. We see that spreading reduces the tail probability and there are tradeoff points around $x = 15$. Although the performance of state-dependent routing schemes are sensitive to the variability of traffic, we see that combining a proactive spreading scheme can reduce such sensitivity.

IX. Conclusion and Future Work

In this paper we propose a simple model for the spatial distribution of energy burdens in a multihop ad hoc wireless network. Our primary contribution is to use these models to investigate the design and potential benefits of proactive energy balancing multi-path routing schemes. To do so we develop a simple second order approximation permitting one to investigate tradeoffs of several types, e.g., for ad-hoc networks with or without replenishing and with energy storage capabilities. The essential tradeoff is between the mean and variance of a spatial energy (flow) balancing scheme. For our proposed models one might attempt to identify Pareto optimal energy balancing strategies, e.g., one minimizing the variance subject to a mean energy constraint, or conversely one minimizing the mean energy burden subject to a variance constraint. To simplify matters we consider flow/energy balancing on regular grid model for a simple parameterized family of spreading schemes. This permits us to concretely evaluate how this tradeoff should be optimized for the various network types and possible design criteria. The results are insightful but perhaps not unexpected. For networks with increased energy storage and/or replenishing capabilities it pays to be more aggressive in spreading traffic so as to reduce the variance in the energy burden since the additional energy burden can be smoothed by energy reserves or new energy sources – one must however ensure that the energy burden does not exceed the replenishing capability. For the most part our simulations

confirm our analytical results and permitted us to evaluate more general regimes of interest.

We note however that the traffic patterns and network geometry used in our simulations are fairly benign in that they are fairly homogeneous in time and space. In practice, one would expect to see irregular topologies and imbalances and variability in traffic loads. These in turn would lead to additional variability in the energy burdens on the network. We expect, that the benefits of proactive load balancing to be be more prominent and sensitive to design in the presence of the aforementioned fluctuations. The degree of spreading, e.g., w, might advantageously be exploited to adaptively smooth out such spatial variabilities and achieve improved balancing of energy burdens coupled with improved performance on network lifetime.

Finally we note that our focus here has been on a preliminary analysis of proactive energy balancing. As such we have used a simplified energy model, appropriate to study a routing scheme. Yet overheads associated with setting up multi-path routes, or other sources of energy expenditure or savings, e.g., putting nodes to sleep, will play a role. For example, in our model we have for the most part ignored MAC layer. In practice the temporal granularity on which load balancing is performed might be critical. For example, fine grain spreading of traffic might cause contention for transmission among neighboring paths lessening the benefits from an energy perspective. Such interactions need to be studied carefully, and might be lessened by increasing the granularity of spreading. These and additional aspects of the proposed routing strategies are part of our ongoing work.

APPENDIX

Proof of Lemma 2: We consider only the left half part of the geometry using the symmetric property of the problem. Let U be the grid set of the left half part, i.e. $U := \{(i,j) \mid 0 \le i \le l/2,\ |j| \le \frac{w-1}{2}\}$. We have that

$$\sum_{i,j \in U} e_{i,j}^2 = \left\{ \sum_{k=0}^{(w-1)/2} \sum_{|i|+|j|=k} e_{i,j}^2 \right\} \quad (21)$$

$$+ \sum_{|i|+|j|>(w-1)/2} \{e_{i,j}^2\} \quad (22)$$

We minimize the summation in two parts, (21) and (22). For (21), when $k=1$, the inner summation is $e_{1,0}^2 + e_{0,1}^2 + e_{0,-1}^2$. Since the flows at $(1,0),(0,1),(0,-1)$ are originated from the source at $(0,0)$, the sum of the total outgoing flows at these locations must sum up to 1, i.e., $e_{1,0} + e_{0,1} + e_{0,-1} = 1$ by the flow conservation. Then by Cauchy-Schwarz inequality, we have that

$$e_{1,0}^2 + e_{0,1}^2 + e_{0,-1}^2 \ge \frac{1}{3}\{e_{1,0} + e_{0,1} + e_{0,-1}\}^2 = \frac{1}{3},$$

and this holds when $e_{1,0} = e_{0,1} = e_{0,-1} = \frac{1}{3}$. Similarly,

$$\sum_{|i|+|j|=k} e_{i,j}^2 \ge \frac{1}{2k+1} \left\{ \sum_{|i|+|j|=k} e_{i,j} \right\}^2,$$

and the equality is achieved when $e_{i,j} = \frac{1}{2k+1}$.

For (22), it can be shown that the minimization is achieved by setting all $e_{i,j}$ equal to $\frac{1}{w}$ due to the constraint (14). We refer the reader to [8] for the proof.

■

Proof of Theorem 3: We have that the energy request arrival process is Poisson with rate λ per unit time per unit space. Since S_i is defined as the energy request in unit time interval, S_i is stochastically equivalent to the shot-noise process in $\mathbb{R}^2$ with intensity λ. From Lemma 1, the n-th order cumulant of S_i is $\chi^{(n)}(1)$, thus we have that

$$\begin{aligned} C(\theta) &= \sum_{n=1}^{\infty} \chi^{(n)} \frac{\theta^n}{n!} = \lambda \sum_{n=1}^{\infty} E[\int_{\Phi_0} h(x,\Phi_0)^n dx] \frac{\theta^n}{n!} \\ &= \lambda E[\int_{\Phi_0} \sum_{n=1}^{\infty} h(x,\Phi_0)^n \frac{\theta^n}{n!} dx] \\ &= \lambda E[\int_{\Phi_0} \{e^{\theta h(x,\Phi_0)} - 1\} dx]. \end{aligned}$$

■

REFERENCES

[1] V. Rodoplu and T. Meng, "Minimum energy mobile wireless networks," *IEEE Jounal on Selected Areas in Communications*, vol. 17, no. 8, pp. 1333–1344, August 1999.

[2] J. Chang and L. Tassiulas, "Maximum lifetime routing in wireless sensor networks," in *Proceedings of Advanced Telecommunications and Information Distribution Research Program, College Park, MD*, 2000.

[3] C. Toh, H. Cobb, and D. Scott, "Performance evaluation of battery-life-aware routing schemes for wireless ad hoc networks," in *Proceedings of ICC*, 2001.

[4] S. Servetto and G. Barrenechea, "Constrained random walks on random graphs: Routing algorithms for large scale wireless sensor networks," in *Proceedings of the 1st ACM International Workshop on Wireless Sensor Networks and Applications*, 2002.

[5] D. Dobkin, S. Friedman, and K. Supowit, "Delaunay graphs are almost as good as complete graphs," *Discrete & Computational Geometry*, vol. 5, pp. 399 – 407, July 1990.

[6] F. Baccelli, K. Tchoumatchenko, and S. Zuyev, "Markov paths on the Poisson-Delaunay graph with applications to routing in mobile networks," *Adv. Appl. Probab.*, vol. 32, pp. 1–18, 2000.

[7] L. Heinrich and V. Schmidt, "Normal convergence of multidimensional shot noise and rates of this convergence," *Adv. Appl. Prob.*, vol. 17, pp. 709–730, 1985.

[8] S. Baek and G. de Veciana, "Spatial energy balancing in large-scale multi-hop wireless networks," Tech. Rep., Wireless Networking and Communications Group (WNCG), UT at Austin, Technical Report, 2004.

[9] S. Nash and A. Sofer, *Linear and Nonlinear Programming*, McGraw-Hill, New York, 1996.

[10] R. Adler, *The Geometry of Random Fields*, Wiley, New York, 1981.

[11] D. Aldous, *Probability approximations via the Poisson clumping heuristic*, Springer-Verlag, New York, 1989.

[12] J. Cohen, "The M/G/1 fluid model with heavy-tailed message length distributions," Tech. Rep. PNA-R9714, Centrum voor Wiskunde en Informatica, Technical Report, 1997.

[13] W. Whitt and P. Glynn, "Logarithmic asymptotics for steady-state tail probabilities in a single-server queue," *Studies in Applied Probability, Papers in Honour of Lajos Takacs, J. Galambos and J. Gani (eds.), Applied Probability Trust*, pp. 131 – 156, 1994.

[14] X. Su and G. de Veciana, "Predictive routing to enhance qos for stream-based flows sharing excess bandwidth," *Computer Networks*, , no. 42, pp. 65–82, May 2003.